2.5 RF Systems

2.5.1 Introduction

RF system requirements

The ERL main Linac superconducting cavities operate in a regime with zero beam loading (in the absence of errors) as the decelerated re-circulating beam cancels the beam loading of the accelerated beam. This essential feature of an ERL allows one to operate these cavities at a high external quality factor, ideally equal to the cavity intrinsic quality factor, to minimize the RF power requirements. However, taking into account such factors as the cavity detuning due to environmental noise (microphonics) and the accelerator return loop path length fluctuations, significantly increases the RF power demand [1]. Other factors, such as the power required to compensate for beam loss in the return loops or additional power required during the beam ramp-up, contribute significantly less to the overall power budget and are not considered here.

To analyze the effects under consideration, it is convenient to use a formula for the RF generator power from [2]. In a slightly modified form, taking into account that the beam now consists of two beams – accelerating and decelerating – and neglecting beam losses and second order terms, the formula for the RF power P_{forw} required to maintain a given accelerating voltage V_{acc} in the ERL cavities is

$$P_{forw} = \frac{V_{acc}^2}{4 \cdot R/Q \cdot Q_L} \cdot \frac{\beta + 1}{\beta} \left\{ 1 + \left(2Q_L \cdot \frac{\Delta\omega}{\omega_c} + \frac{I_b R/Q \cdot Q_L}{V_{acc}} \cdot \Delta\phi \right)^2 \right\} \tag{2.5.1}$$

$$Q_L = \frac{Q_0}{\beta + 1} = Q_{ext} \frac{\beta}{\beta + 1} \tag{2.5.2}$$

where R/Q is the ratio of cavity shunt impedance R to its intrinsic quality factor Q_0, Q_L is the loaded quality factor, and Q_{ext} is the external quality factor of the input power coupler. β is the coupling coefficient, I_b is the accelerating beam current, $\Delta\omega = \omega_c - \omega$ the peak cavity detuning caused by microphonics, and $\Delta\phi$ is the decelerating beam phase error due to fluctuations in the return loop path.

Considering only the effect of microphonic noise:

$$P_{frow} = \frac{V_{acc}^2}{4 \cdot R/Q \cdot Q_L} \cdot \frac{\beta + 1}{\beta} \left\{ 1 + \left(2Q_L \cdot \frac{\Delta\omega}{\omega_c} \right)^2 \right\} \tag{2.5.3}$$

From this equation, the maximum power is determined by the peak cavity detuning, and for each value of peak detuning, there is an optimal external quality factor that minimizes the required RF power as illustrated in Fig. 2.5.1.

Experience at several laboratories [3] indicates that achieving peak microphonics detuning of less than 10 Hz is possible. On the other hand, the same experience and the measurements on the ERL injector prototype [4] have shown significant cavity-to-cavity and cryomodule-to-cryomodule spread in this noise level. Based on these facts, typical peak detuning due to microphonics is assumed to be 10 Hz. Allowing for the variation of detuning from cavity to cavity, the maximum peak detuning is taken as 20 Hz. The optimal value of the external

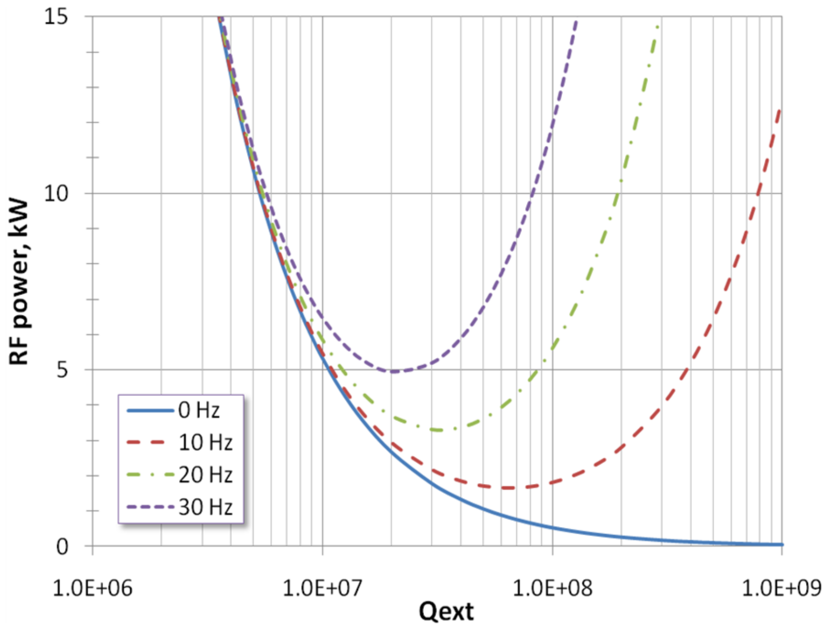

Figure 2.5.1: Required RF power to maintain an accelerating gradient of 16.2 MV/m in a 7-cell main Linac cavity as function of the coupler external quality factor for different peak microphonic detuning (no re-circulating beam phase errors).

quality factor of 6.5×10^7 was chosen for the typical peak detuning. For this Q_{ext} and maximum detuning of 20 Hz, the required peak power is 4.12 kW and the average power is 1.22 kW.

Next consider the effect of a small phase error $\Delta\phi$ of the re-circulating beam. While a DC component of this error or a slow phase drift can be exactly cancelled by the appropriate cavity detuning, fast fluctuations would require additional RF power to counteract. To keep the required peak RF power below 5 kW, the peak $\Delta\phi$ should be less than 0.1°. Cavity field amplitude and phase stability requirements are derived following the analysis presented in [1]. Table 2.5.1 summarizes main requirements to the Linac RF system.

State of the art

All existing RF systems for L-band CW SRF Linacs – CEBAF and the FEL at Jefferson Laboratory, ALICE at the Daresbury Laboratory, ELBE at HZDR (Dresden-Rossendorf) – employ a simple scheme with one cavity per High Power RF Amplifier (HPA). This scheme provides better cavity field amplitude and phase control, more operational flexibility, and better RF system efficiency. It was also in part dictated by available RF power sources.

Three types of high CW RF power generating devices are available from industry: klystrons, inductive output tubes (IOTs), and solid state amplifiers. Their applications in accelerators are summarized in [5–7]. Klystrons have traditionally been used in the past and they are still the technology of choice at higher power levels. However, they are highly non-linear devices if operated close to saturation and their efficiency drops very quickly at reduced output power. It is worth noting that the largest presently operating CW superconducting Linac RF system

Table 2.5.1: Main requirements to the Linac RF system

Operating frequency	1.3 GHz
Number of 7-cell cavities	384
Accelerating gradient	16.2 MV/m
Accelerating voltage per cavity	13.1 MV
R/Q (circuit definition)	400 Ω
Q_{ext}	6.5×10^7
Peak detuning due to microphonics	20 Hz
Typical detuning due to microphonics	10 Hz
Peak RF power per cavity	5 kW
Average RF power per cavity	< 2 kW
Amplitude stability	1×10^{-4} rms
Phase stability	0.05° rms

in the world, CEBAF, uses 1497 MHz klystrons. The CEBAF klystrons operate very reliably with an average lifetime of 165,000 hours [8]. Analysis for the CEBAF 12 GeV Upgrade RF showed no overall cost savings for IOT-based amplifiers over klystron-based ones [9] and the klystron technology has been chosen for the upgrade RF system.

IOTs currently have practically replaced klystrons in the TV broadcast industry and are also offered in L-band by several manufacturers. The main advantages of IOTs over klystrons are higher efficiency ($>$ 60% at maximum output power), the absence of saturation, higher linearity (but not at low power levels), smaller size, and lower cost per tube. The disadvantages are lower gain, non-linear behavior at low power levels, and limited output power. While no large-scale installations of L-band IOTs exist and no long-term reliability data are available, several tubes are in service around the world. These tubes are at the Cornell ERL injector prototype, ALICE (Daresbury Laboratory), ELBE (HZDR, Dresden-Rossendorf), HoBiCaT (HZB), and the ERL prototype (KEK). The latest available statistics from industry (one manufacturer) on broadcast IOTs is from 2007. At that time, the mean time before failure (MTBF) was reaching 42,230 hours with some tubes having maximum operating hours of more than 70,000 hours. The statistics were for 343 tube positions and are expected to improve over time as many of the originally installed tubes were still operational and hence not included in the calculations.

Following recent advances in high-power transistor technology, solid-state amplifiers are being adopted for high-power RF systems in accelerators. In the past, the efficiency of solid-state amplifiers was much worse than that of the other two technologies, but recently manufacturers have begun to specify typical RF efficiencies up to 50% with an overall system efficiency (including DC power supplies) of 42% [10]. This is approaching that of IOT and klystron-based amplifier systems. A prototype 10 kW solid-state amplifier was recently installed and commissioned at HZDR (Dresden-Rossendorf) [11]. The advantages of solid-state amplifiers are low power supply voltage, graceful degradation, and easier maintenance due to their modular design. It is important to note, that due to their modular design, a single, output-power-transistor failure does not cause complete system failure and only reduces the available output power.

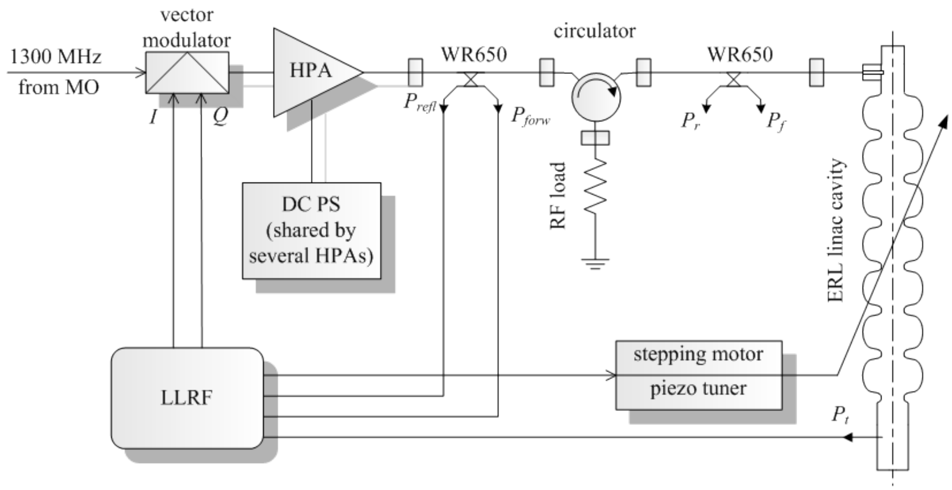

Figure 2.5.2: Block diagram of an RF channel for the ERL main Linac.

Table 2.5.2: Main specifications for the ERL Linac RF HPA.

Frequency	1.3 GHz
Peak output RF power	$\geq$ 5 kW
Average output RF power	$\geq$ 2 kW
Bandwidth at 1 dB points (min.)	$\pm$1.5 MHz
Bandwidth at 3 dB points (min.)	$\pm$2.5 MHz
RF phase pushing (0.03 kW to 5 kW output power)	$< 7°$
Gain change (0.03 kW to 5 kW output power)	$<$ 3 dB
RF output amplitude ripple (0.03 kW to 5 kW output power)	$<$ 0.2% rms
RF output phase ripple (0.03 kW to 5 kW output power)	$< 0.5°$ rms
Efficiency at 5 kW	$\geq$ 50%
Efficiency at 2 kW	$\geq$ 40%

2.5.2 Architecture of the main Linac RF

The ERL main Linac RF system consists of 64 RF stations (35 in the north Linac and 29 in the south Linac) with one station per cryomodule. One station is comprised of six independent RF channels (one per cavity), each including a HPA, Low Level RF (LLRF) controls, interlocks and monitoring electronics, and a waveguide or rigid coaxial transmission line connecting the HPA to the cavity fundamental power coupler. A three-stub tuner can be inserted in the transmission line for Q_{ext} adjustment if necessary. One or more DC power supplies are shared by the station's HPAs. All components of the RF stations will be installed in the Linac tunnel in radiation-shielded enclosures. Figure 2.5.2 shows a basic block diagram for one RF channel.

2.5.3 High-power RF: Choice of the RF technology and Phase 1b efforts

The Linac RF HPAs will be located in the Linac tunnel at the SRF cryomodules. To satisfy the requirements outlined in §2.5.1 and the limited space in the tunnel, the HPA must be a compact, modular, highly efficient, linear, high-gain amplifier. Such an amplifier should meet the specifications listed in Table 2.5.2. The solid-state technology was chosen for the baseline design due to its advantages particularly with regards to linearity, complexity, size and cost. We are therefore in the process of testing a 5 kW, 1.3 GHz solid state amplifier. However, issues regarding reliability and radiation hardness require further investigation before a final decision is made. These issues will be explored during Phase 1b. A prototype unit will be ordered from industry, thoroughly tested off line and then used in a main Linac cryomodule high-power test. Based on the test results, a final decision will be made on which technology to choose for HPA.

2.5.4 Low level RF

Master oscillator and reference signal distribution

The 1.3 GHz reference signal required for cavity regulation is generated by the master oscillator. In the simplest case, the master oscillator uses an RF oscillator with a resonant frequency of 1.3 GHz [12], which is phase-locked to a quartz oscillator and/or a rubidium transition to provide sufficient long-term stability. The required timing stability of the master oscillator depends strongly on the ERL operation mode. In the 100 mA operation mode with its 2 ps (rms) long bunches, a timing stability of 200 fs is required corresponding to $1/10^{\text{th}}$ of the bunch duration. Master oscillators operating at 1.3 GHz offering a better frequency stability than this already exist, for example at FLASH [13].

The required distribution length for the 1.3 GHz signals is around 500 m, which would still barely be possible via coaxial cables in terms of cable losses. Alternatively, a lower frequency could be distributed, allowing for lower transport losses, and the 1.3 GHz signals would then be generated by phase locking local 1.3 GHz oscillators to this distributed signal. Both of these schemes could deliver long-term stability in the picosecond range, which might be sufficient for the 2 ps bunch mode of the ERL, especially, if beam-based feedback loops are used to compensate for cable drifts.

The short-pulse operation mode with its sub-100 fs bunches will require significantly improved stability, which can be achieved with the optical synchronization schemes as discussed in the beam diagnostics and controls section.

Low level RF system

The objectives of the LLRF control system are to stabilize the accelerating fields in the main Linac cavities, and to provide excellent operability, availability, and maintainability. The design of the LLRF system is driven by the following requirements:

- A compact, cost-effective design is essential, since all of the LLRF electronics will be placed in the main Linac tunnel, and space is limited.

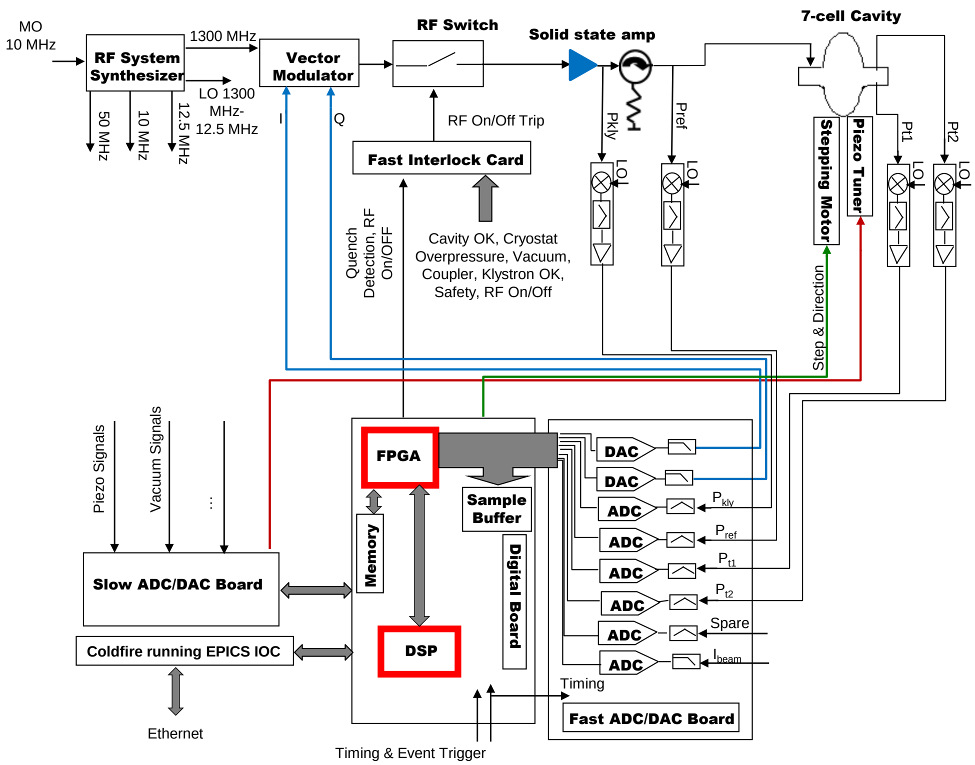

Figure 2.5.3: Block diagram of the main Linac LLRF system for a single cavity. Shown are both the RF hardware (RF synthesizer, vector modulator, solid state amplifier, down-converters) and the digital hardware (fast ADC/DAC board, main digital processor board, slow ADC/DAC board, EPICS IOC processor board). A fast, analog interlock provides protection in addition to the digital trip detection.

- The LLRF electronics will be in a radiation producing environment (x-rays and neutrons).
- No direct access to the electronics will be available during operation of the accelerator.
- The RF fields in the cavities need to be stabilized to $\sigma_A/A = 10^{-4}$ in relative amplitude and $\sigma_p = 0.05°$ in phase.
- Efficient main Linac cavity operation requires operating at high loaded-quality factors of 6.5×10^7 and above.

These requirements resulted in the design described below. Figure 2.5.3 shows the block diagram of the main Linac LLRF system. Operation at very high-loaded quality factors requires operating each cavity from an individual RF power source. Accordingly, there will be an individual LLRF system for each main Linac cavity. A digital LLRF system will be used since it allows running the complex feedback and feed forward loops while providing easy integration of diagnostics and data logging. All RF signals (forward power, reflected power, and the cavity field probe signal) will be down-converted to an intermediate frequency and then 4 times oversampled by analog-to-digital converters (ADC) to give a complex phasor representing the amplitudes and relative phases of the RF signals. Very fast digital components like Field-Programmable Gate Arrays (FPGAs) will be used to achieve very low feedback loop latency $< 1\,\mu$s, allowing high feedback gains of several thousand to achieve sufficient field stability in the presence of the strong field perturbations mentioned above. The large phase perturbations by cavity microphonics make an in-phase quadrature (IQ) field feedback controller the preferred choice over of a traditional amplitude and phase controller. A digital filter will be used to avoid feedback loop instabilities caused by the $6/7\ \pi$ TM010 mode. The fast feedback loops stabilizing the RF cavity field will be accompanied by feedback and feedforward loops controlling the cavity frequency. These slower loops will compensate the change in cavity frequency due to the Lorentz force detuning when the field amplitude is changed (for example during turn-on of the cavity fields), and partly compensate the cavity detuning by microphonics. Sophisticated trip detection and a state machine will provide protection, exception handling, automated calibrations, cavity turn-on and trip recovery.

The RF and digital hardware for a single cavity will be packaged into a compact LLRF unit in order to minimize the impact on accelerator operation. Problems of a failed unit can be diagnosed and repaired off-line, and the impact on the availability of the accelerator minimized. The radiation environment will be addressed in several ways . Radiation shielding will be used to reduce x-rays and neutrons to an acceptable level at the LLRF electronics. Estimates of the expected radiation level in the ERL main Linac tunnel have shown that this is achievable with modest radiation shielding. In addition, where required, radiation-hard electronic components will be used. Single-event upsets by neutrons will be diagnosed by running two identical copies of the digital control loops in parallel. If a bit in one of the loops is changed by a neutron, the results of the two control loops will disagree. A re-flash of the digital components on that given cavity unit will then be used to repair such single event upsets.

The digital IQ LLRF system built for the Cornell ERL injector serves as a prototype for the LLRF system of the main Linac [14]. Figure 2.5.4 shows the digital processor board of this system together with a block diagram of its digital components. The prototype LLRF system has all the functionallity needed for the main Linac and meets the performance specifications given above. The final version will have a more compact form factor and will employ a hardware platform with very high reliability, e.g. a modified version of the MicroTCA platform. The prototype LLRF system has been tested extensively with the low-loaded quality factor cavities in the Cornell ERL injector, as well as with very high quality factor cavities both with and without ERL like beam operation. Figure 2.5.5 , Fig. 2.5.6 and Fig. 2.5.7 show some highlights from these LLRF tests.

In a proof of principle experiment, Cornell's digital LLRF system has been connected to one of the 7-cell cavities in the TJNAF ERL-FEL. After an initial test at the standard loaded quality factor of $Q_L = 2 \times 10^7$, the loaded Q_L was increased to a record value of 1.2×10^8. Excellent field stability was achieved with full 5 mA beam current in energy recovery mode(see Fig. 2.5.5) Less than 500 W of driving RF power was required for operation at a gradient of 12.3 MV/m. No dependence of the field stability on beam current (0 to 5.5 mA) and off-crest angle (between -40° and $+40^\circ$) was found. Even at this high loaded Q ,the cavity operated very reliably over several hours without any trips. Piezo tuner based frequency control proved to be very effective in keeping the cavity on resonance during cavity field ramp-up. The Lorentz

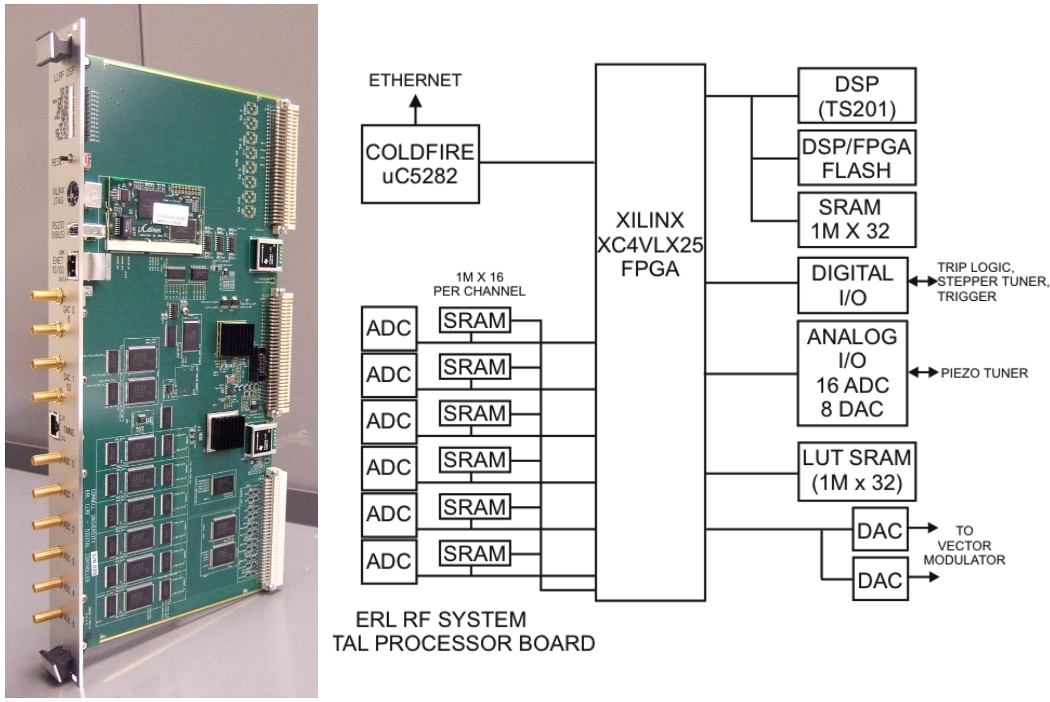

Figure 2.5.4: Digital LLRF system developed for the Cornell ERL injector prototype. Left: Main processor board. Right: Block diagram of the digital boards with the XILINX FPGA and a TigerSHARC DSP. The system uses six 16-bit ADCs running at 50 MHz and two fast 16 bit DACs as analog outputs for field control.

force detuning of the cavity was compensated effectively by the piezo tuner, and allowed ramp-up to high gradients in less than 1 s reliably even at $Q_L = 1.2 \times 10^8$ (see Fig. 2.5.5). This is desirable for fast trip recovery in a large ERL. This described test demonstrates that no fundamental limit prohibits cavity operation at a loaded Q of up to 10^8, and that very high field stability can be achieved at the same time.

In a second test of Cornell's digital LLRF system with a high-loaded Q cavity, the LLRF system was connected to a 9-cell ILC type cavity at the Helmholtz-Zentrum Berlin. The cavity was operated at three different loaded Q values of 5×10^7, 1×10^8, and 2×10^8. In all three cases, excellent field stability in amplitude and phase was achieved by running with proportional feedback gains of several thousand to compensate for the strong field perturbations caused by cavity microphonics ($\sim$ 6 Hz rms, $\sim$ 30 Hz peak) (see Fig. 2.5.6). Feedback control of microphonics cavity detuning has been demonstrated successfully at the Cornell ERL injector cryomodule. The frequency tuners of the 2-cell injector cavities are equipped with fast piezo-electric actuators for fast-frequency tuning. First steps have been taken to explore the potential and robustness of microphonics compensation using these fast tuners in a feedback loop. For robustness, a proportional-integral-derivative (PID) frequency feedback loop was implemented

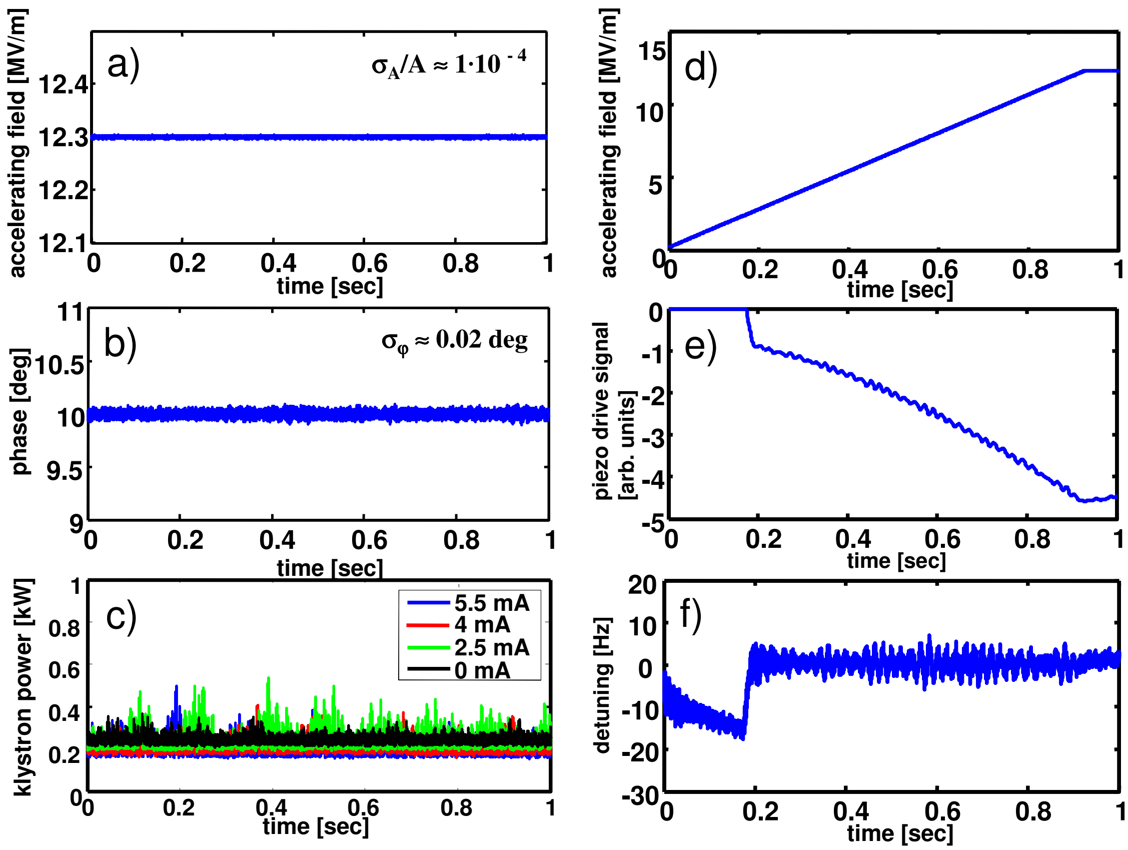

Figure 2.5.5: Results from a test of Cornell's LLRF system at the TJNAF FEL-ERL operating a 7-cell cavity with a high loaded quality factor Q_L of 1.2×10^8. (a-c) CW operation. The field stability is exceeding the Cornell ERL main Linac specifications. (d-e) Cavity filling with piezo tuner based Lorentz-force detuning compensation [15]

with a simple digital filter in the LLRF system. Optimizing the gains and the digital filter provided a 70% reduction in the rms microphonics level (see Fig. 2.5.7).

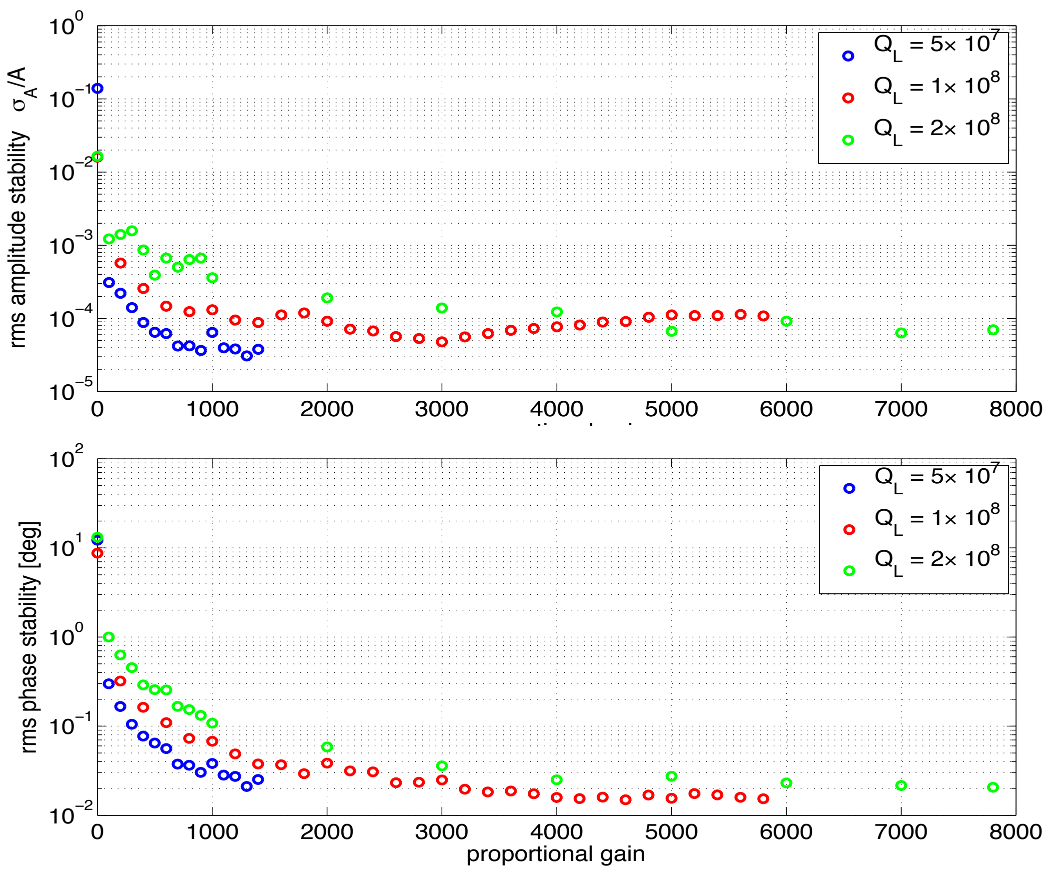

Figure 2.5.6: Amplitude and phase stability as function of proportional gain at different loaded Q_L values of 5×10^7, 1×10^8, and 2×10^8. The RF field in the 9-cell ILC cavity at the Helmholtz-Zentrum Berlin is stabilized by Cornell's digital LLRF system.

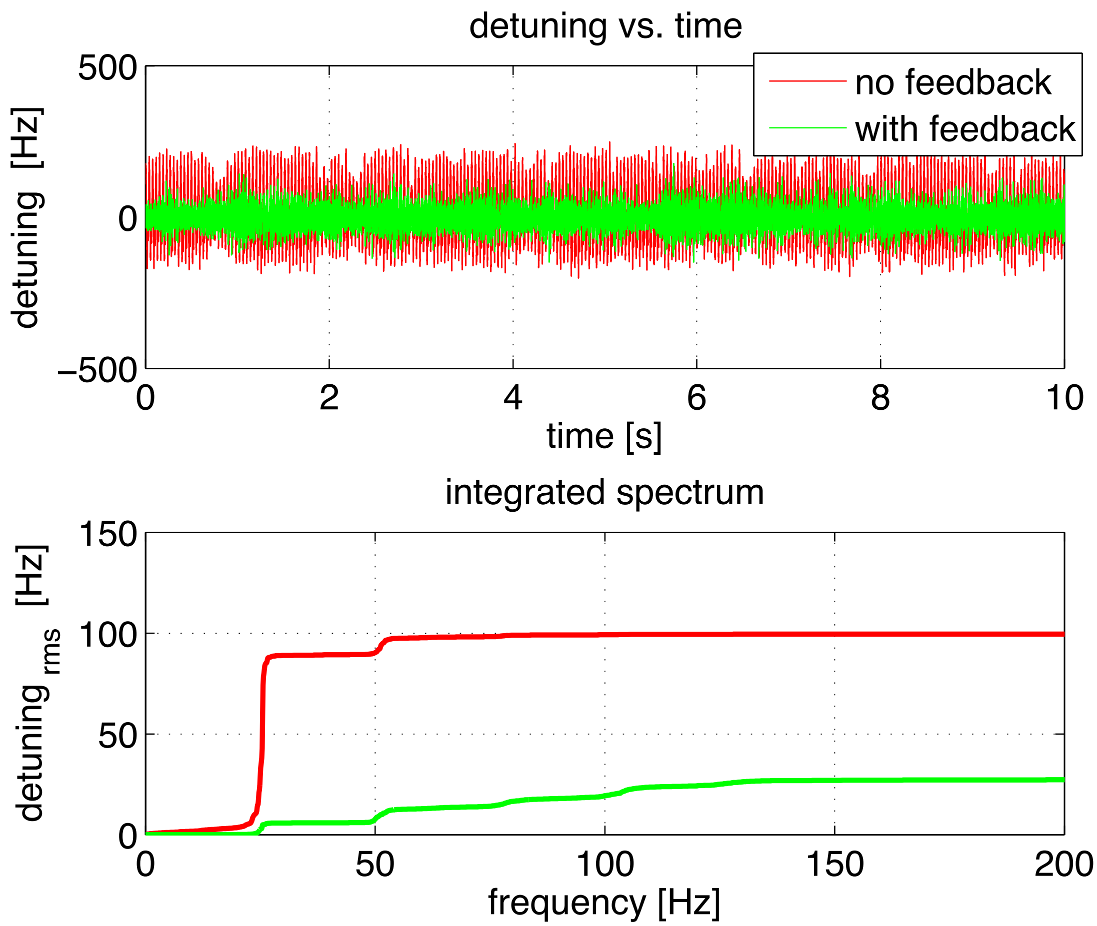

Figure 2.5.7: Microphonics compensation by a fast piezo-electric tuner in feedback mode at the Cornell SRF injector cryomodule. Top: Detuning vs. time with and without compensation. Bottom: Integrated micro- phonics spectrum for the two detuning cased shown above. The feedback loop reduced the microphonics level by $\sim 70\%$.

References

[1] Liepe, M. and S. Belomestnykh. *RF parameter and field stability requirements for the Cornell ERL prototype*. In *Proceedings of the 2003 Particle Accelerator Conference*, pages 1329–1331. Portland, USA (2003).

[2] Wilson, P. B. *High Energy Electron Linacs: Application to StorageRing RF Systems and Linear Colliders*. Technical Report SLAC-PUB-2884, SLAC (1982). http://www.slac.stanford.edu/cgi-wrap/getdoc/slac-pub-2884.pdf.

[3] Liepe, M. and J. Knobloch. *Superconducting RF for energy-recovery linacs*. Nucl. Instr. and Meth. A, **557** (1), pages 354 – 369 (2006). ISSN 0168-9002. doi:DOI:10.1016/j.nima.2005.10.099. Energy Recovering Linacs 2005 - Proceedings of the 32nd Advanced ICFA Beam Dynamics Workshop on Energy Recovering Linacs.

[4] Conway, Z. and M. Liepe. *Electromagnetic and Mechanical Properties of the Cornell ERL Injector Cryomodule*. In *the 23rd Particle Accelerator Conference*, pages 915–917. Vancouver, British Columbia, Canada (2009).

[5] Belomestnykh, S. *RF systems for CW SRF linacs*. In *The XXIV Linear Accelerator Conference*. Vancouver, British Columbia, Canada (2008).

[6] Bohlen, H. and T. Grant. *Vacuum Electron Device Limitations for High-Power RF Sources*. CWRF2008 Workshop on High Power RF (2008). http://cwrf08.web.cern.ch/cwrf08/.

[7] Caplot, M., *et al. New generations of RF amplifiers: from gridded tubes to dual technology solutions*. CWRF2008 Workshop on High Power RF (2008). http://cwrf08.web.cern.ch/cwrf08/.

[8] Walker, R. and R. Nelson. *Operating Experience and Reliability Update on the 5 kW CW Klystrons at Jefferson Lab*. CWRF2008 Workshop on High Power RF (2008). http://cwrf08.web.cern.ch/cwrf08/.

[9] Hovater, C. *CEBAF Energy Upgrade Low Level RF (LLRF) Activities*. Seminar at Cornell University (2006).

[10] *Preliminary datasheet of BLA10000CW 1300 MHz amplifier* (2010). Bruker BioSpin, private communications.

[11] (2010). Private communications with H. Buettig (HZDR Rossendorf) and P. Dupire (Bruker BioSpin).

[12] Stockwell, P., *et al. A Low Phase Noise 1.3 GHz Dielectric Resonator Oscillator*. http://psi.com.au/media/pdfs/FSC2006%20-%201-3%20GHz%20Dielectric%20Oscillators.pdf.

[13] Simrock, S., *et al. Performance of the new master oscillator and phase reference system at FLASH*. In *the twenty-second Particle Accelerator Conference*, pages 188–190. Albuquerque, New Mexico, USA (2007).

[14] Liepe, M. In *Proceedings of the 2003 Particle Accelerator Conference*. Portland, Oregon, USA (2003).

[15] Liepe, M. In *the 2005 Particle Accelerator Conference*. Knoxville, TN, USA (2005).